EVALUATION OF A SUB-GRID MODEL IN A TURBULENT CIRCULATING FLUIDIZED BED

Ivan Carlos Georg
SINMEC – Laboratory of Numerical Simulation in Fluid Dynamics and Computational Heat Transfer
Dept. of Mechanical Engineering
Federal University of Santa Catarina
Postal Office Box 476
Zip Code: 88040-900 Florianopolis, SC, Brazil
ivan@sinmec.ufsc.br

Clovis R. Maliska
SINMEC – Laboratory of Numerical Simulation in Fluid Dynamics and Computational Heat Transfer
Dept. of Mechanical Engineering
Federal University of Santa Catarina
Postal Office Box 476
Zip Code: 88040-900 Florianopolis, SC, Brazil
maliska@sinmec.ufsc.br

Luismar Marques Porto
Dept. of Chemical Engineering
Federal University of Santa Catarina
Florianopolis, SC, Brazil
luismar@enq.ufsc.br

Abstract. *The 3D transient hydrodynamics of gas-solid flow in a turbulent circulating fluidized bed is numerically studied. The grid refinement is carefuly handled to be adequate for capturing the structures of agglomerated particles (clusters and strands) which are found in the so called meso-scale. A sub-grid model (LES) is applied for the gas phase and extended for the solid phase. The numerical results are compared with the experimental ones with good approximation for the average axial velocities for the solid phase. The sub-grid model employed gives good behavior at near wall and intermediate regions, with deviation in the central region (dilute) by over-estimating the drag. This deviation seems to be caused by the way drag is calculated by the two-fluid model. Spectral analysis is also performed for the studied cases. The inertial region was observed by the spatial and temporal resolutions, to have a -5/3 slope, indicating that the refinement in space and time was adequate.*

Keywords*: two-phase gas-solid flow, turbulence, fluidized bed, clusters, sub-grid models.*

1. INTRODUCTION

Circulating gas-solid fluidized beds (CFB) are common devices found in many operations in the chemical, petroleum, pharmaceutical, agricultural, biochemical, food and power generation industries. The hydrodynamic behavior of fluidized systems is non-linear and therefore very complex. Scale-up from lab-scale to industrial scale, a strong requirement when designing new equipments, is a major problem. The nature of hydrodynamic interactions at various scales in such devices present great challenges when attempting to model them mathematically. The most common practice is to use averaged transport equations for two-phase flows, van Wachem (2000), Zhang and VanderHeyden (2001), Agrawal *et al.* (2001), Huilin *et al.* (2003), among several others. While these efforts presented some success, the estate-of-the-art for two-phase flow simulation is still far from ideal. Meso-scale structures in the form of clusters and strands are commonly observed in dilute gas-particle flows. These structures affect the overall flow behavior, with greatly influences in momentum and energy exchanges, and should therefore be accounted for in computational fluid dynamic (CFD) simulations of CFB's.

Unfortunately, the meso-scale structures cannot be adequately resolved in CFD simulations of typically sized CFB's. The goal of the present study is to evaluate a sub-grid model to account for the effect of the unresolved meso-scale structures in a circulating gas-solid fluidized bed and compare to a well characterized fluidized bed experiment performed by van den Moortel *et al.* (1998). In what follows, we discuss some background on the averaged equations for two-phase gas-solid flows and present the sub-grid model used and the results compared with experiment.

2. CONTEXT OF THE GAS-SOLID FLOW PROBLEM

Computational fluid dynamics (CFD) is an emerging technique for predicting the flow behavior of many systems required scale-up, design or optimization. Although single-phase CFD tools are widely and successfully applied

(Anderson, 1995), multiphase flow remains unresolved due to the complex mathematics and the difficulty in the physical description (van Wachem, 2000).

CFD models for gas-solid flow can be divided into two groups, Lagrangian and Eulerian models. Lagrangian models or discrete particle models, calculate the path of each individual particle. The interaction between the particles can be described by a potential force and by collision dynamics. The drawbacks of the Lagrangian technique are the large memory requirements and the large calculation time. Moreover, the description of the drag force from the gas phase acting on each particle is difficult to model accurately, and this is in practice based on experimental correlations. In other words, it is impossible to track all gas/solid interfaces which exist in a real flow.

Eulerian models treat the particle phase as a continuum performing an average on the scale of individual particles. Computations by this method can predict the behavior of dense-phase flows on a realistic geometry, van Wachem (2000). The drawback of this method, however, is that one requires complex statistics to translate the behavior of many particles into one continuum. For this purpose, often granular kinetic theory is generally employed. At a basic level, interactions between the fluid and particles are simply modeled with a drag force.

As we know from single-phase flow, the nonlinearity of the convective term in the momentum equation gives rise to the Reynolds turbulence tensor. In two-phase flow, there are additional nonlinearities that rise from the mass-momentum coupling in both the mass and momentum conservation equations, Zhang and van der Heyden (2001). Both these nonlinearities give rise to meso-scale phenomena called particle clustering in which particles aggregate into dynamic structures with higher than average volume fraction of solids. This phenomenon is observed both experimentally and numerically.

Cluster formation is observed in fine-grid (5-10 particle diameters (Agrawal *et al.* 2001 and 50-100 particle diameters (Zhang and van der Heyden, 2001, Georg, 2005). When the fine grid calculation results are averaged and compared with coarse-grid calculations results, different flow fields are obtained. Coarse-grid calculations filter out the meso-scale effects. Because of the meso-scale effects influence the macro scale behavior, they should be properly taken into account in the coarse-grid calculations by use of appropriate sub-grid model for the apparent viscosity, for example. Horio and Kuroki (1994) measured the typical cluster diameter which was 10-100 times the particle diameter.

The downward motion of a cluster causes a major variation in the local velocity profile and should therefore lead to a significant increase in the production of gas-phase turbulence arising form stiff gradients in mean velocities, Geraldine *et al*. (2004) and Georg (2005). This idea is supported by the computational data of Agrawal *et al*. (2001), in which a strong increase in gas-phase turbulence production resulting from cluster formation was found. Clustering can increase the gas-phase turbulence through other mechanisms as well. Because the effective cluster diameter is large, the cluster will interact with the gas similarly to a large particle, even if only temporarily. It is known that a large diameter particle can significantly enhance the gas-phase turbulence through the vortex-shedding mechanism and through the formation of temporary wakes behind the (larger) particles or the clusters, Geraldine *et al*. (2004). Another mechanism is by the vortex stretching associated with the small areas available for the gas flow caused by cluster formation near wall, Georg (2005).

The purpose of the present study was to better understand the basic behavior of the simple gas-solid flow equations before introducing any particle-particle interactions models. By comparing numerical results with experimental data we are able to make some quantitative assessment of the adequacy of the simple gas-solid flow equations and the sub-grid model proposed. We also use transient high resolution simulations to attempt to fully resolve the meso-scale structures in the flow.

3. AVERAGED EQUATIONS FOR TWO-PHASE FLOWS

The majority of the authors, to obtain the governing equations for multiphase flows, refer to the pioneering work of Anderson and Jackson (1967) or Ishii (1975). Anderson and Jackson (1967) and Jackson (1997) use a formal mathematical definition of local mean variables to translate the Navier-Stokes equations for the fluid and the Newton's equation of motion for a single particle directly into continuum equations representing momentum balances for the fluid and solid phases. The local variables are averaged over regions large with respect to the particle diameter but small with respect to the characteristic dimension of the complete system, to account for variations in the domain. The averaging procedures, (see Jackson, 2000), can be applied to the equations of motion. Starting with the equation of mass conservation, for a incompressible fluid, it takes the form

$$\frac{\partial}{\partial t}\left(r_g f_g\right)+\nabla\bullet\left(r_g f_g \mathbf{U}_g\right)=0\,, \tag{1}$$

For the solid phase, one has

$$\frac{\partial}{\partial t}\left(r_s f_s\right)+\nabla\bullet\left(r_s f_s \mathbf{U}_s\right)=0\,, \tag{2}$$

where f_g and f_s are the volume fractions for the gas and particle phases and $\mathbf{U}_g$ and $\mathbf{U}_s$ are the averaged velocities of the gas and particle phases. The resulting momentum balances for the fluid and solid phases are as follows

$$\frac{\partial}{\partial t}\left(r_g f_g \mathbf{U}_g\right)+\nabla\bullet\left(r_g f_g \mathbf{U}_g \mathbf{U}_g\right)=-\nabla P_g+\nabla\bullet\left[\mathbf{t}_g\right]+f_g r_g \mathbf{g}+b\left(\mathbf{U}_s-\mathbf{U}_g\right) \tag{3}$$

$$\frac{\partial}{\partial t}\left(r_s f_s \mathbf{U}_s\right)+\nabla\bullet\left(r_s f_s \mathbf{U}_s \mathbf{U}_s\right)=-\nabla P_s+\nabla\bullet\left[\mathbf{t}_s\right]+f_s r_s \mathbf{g}+b\left(\mathbf{U}_g-\mathbf{U}_s\right). \tag{4}$$

The first term on the right hand of the gas phase of motion represents the gas pressure, the second term is the averaged shear tensor of the gas phase, the third term represents the gravity force and the forth term is the traction exerted on the gas phase by the particle, the drag force. The first term on the right hand side of Eq. (4) is the solid pressure, the second term is the averaged shear tensor of the solid phase the third term represents the gravity force on the particles and the forth term is the drag force contribution to the solid phase.

The gas stress was calculated using conventional Newtonian form and a modified one using Smagorinsky-like sub-grid model as follows

$$\left[\mathbf{t}_g\right]=m_{g,e} f_g\left[\nabla\mathbf{U}_g+\nabla\mathbf{U}_g^T\right]-\frac{2}{3}m_{g,e} f_g\left[\nabla\bullet\mathbf{U}_g\right]\bar{\bar{\mathbf{I}}}, \tag{5}$$

$$m_{g,e}=m_g+r_g\left(0{,}1\Delta\right)^2\left(\mathbf{t}_g\bullet\mathbf{t}_g\right)^{1/2},\quad \Delta=\left(\Delta x\Delta y\Delta z\right)^{1/3} \tag{6}$$

where $m_{g,e}$ is the effective viscosity of the gas phase modeled by a Smagorinsky sub-grid model and m_g is the gas phase viscosity . In the same way for the particle solid phase, one has

$$\left[\mathbf{t}_s\right]=m_{s,e} f_s\left[\nabla\mathbf{U}_s+\nabla\mathbf{U}_s^T\right]-\frac{2}{3}m_{s,e} f_s\left[\nabla\bullet\mathbf{U}_s\right]\bar{\bar{\mathbf{I}}} \tag{7}$$

$$m_{s,e}=m_s+r_s\left(0{,}1\Delta\right)^2\left(\mathbf{t}_s\bullet\mathbf{t}_s\right)^{1/2},\quad \Delta=\left(\Delta x\Delta y\Delta z\right)^{1/3} \tag{8}$$

where $m_{s,e}$ is the effective viscosity of the solid phase and m_s is the solid phase viscosity and Δ is the filter width. The solid pressure are given by Gidaspow (1994) relations

$$\nabla P_s=G(f_s)\nabla f_s,\qquad G(r_s)=\frac{\partial P_s}{\partial f_s}, \tag{9}$$

$$G(f_s)=G_0\exp\left(-c(f_s-f_{\max})\right), \tag{10}$$

where $f_{\max}=0{,}637$, $G_0=1\,Pa$, $c=600$. c is the fictitious speed of sound for the particle material when it is closely packed, and $f_{\max}$ is the close packing volume fraction for particles. The effect of particle pressure gradient term is to keep the particles apart so that the calculated particle concentration does not exceed the maximum concentration obtainable for a given size distribution of the particles. The gas-solid inter-phase drag coefficients, Gidaspow (1994), are

$$b_{g,s}=\frac{3}{4}C_D\frac{r_g f_s\left|\mathbf{U}_g-\mathbf{U}_s\right|}{d_p}f_g^{-1{,}65},\quad f_g\geq 0{,}8 \tag{11}$$

$$b_{g,s}=\frac{3}{4}C_D\frac{150 f_s^2 m_g}{d_p^2 f_g}+1{,}75\frac{r_g f_s\left|\mathbf{U}_g-\mathbf{U}_s\right|}{f_g d_p},\quad f_g<0{,}8 \tag{12}$$

$$C_D = \frac{24}{\mathrm{Re}}\left(1 + 0{,}15\,\mathrm{Re}^{0{,}687}\right) \quad \mathrm{Re} < 1000, \quad C_D = 0{,}44 \quad \mathrm{Re} \geq 1000. \tag{13}$$

$$\mathrm{Re} = \frac{r_g f_g \left|U_g - U_s\right| d_p}{m_g}. \tag{14}$$

Where d_p is the particle diameter. Equations (1-14) are known as the "Two Fluid Model" and it models an isothermal gas-solid two-phase flow. In the solid and gas phases a Smagorinsky like sub-grid model is incorporated in one of the simulated cases (Case 2).

4. DESCRIPTION OF NUMERICAL SIMULATION

Simulations performed in this study used the geometry described by van den Moortel *et al.* (1998). The cross-section of the fluidized bed is 20x20 cm^2 and the total height is 200 cm. The geometry and grid distribution are illustrated in Fig. 1. The dimension of each volume of the grid was 0.625x0.625x1.33 cm^3, with 153600 volumes.

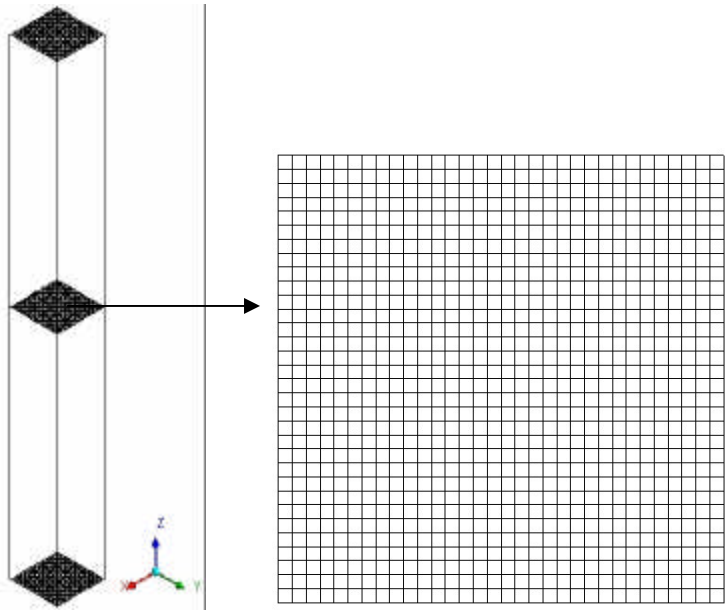

Figure 1. Computational domain and grid.

van den Moortel *et al.* (1998) reported they used particles with mean diameter of 120 μm with standard deviation of the particle diameter of 20 μm. In this paper we ignored the particle size distribution and used the mean diameter. Using this particle diameter we have about 52x52x110 particles enclosed in a x,y,z volume for the grid refinement used. Viscosity of the particle phase was set to be 0.0185 kg/m.s, Gidaspow (1994), and the particle material density r_s was set to be 2400 kg/m^3 as in the experiment. We used a gas density of 1.2 kg/m^3 and viscosity of 1.7 x 10^{-5} kg/m.s.

The numerical simulations were carried out using the CFD code ANSYS CFX 5.6®, which use an element-based finite volume scheme. We implemented the sub-grid model in the multiphase code version of CFX 5.6® using higher resolution scheme for space discretization and a second order backward difference scheme for the time discretization. The time step used for all simulations was $1x10^{-3}$ seconds.

In the simulations, the boundary condition on the solid walls was treated as no-slip for both phases. Generally the free slip boundary conditions are used for the solid phase. Jackson (2000) suggests as boundary condition for de solid phase an energy balance. Andrews *et al.* (2005) conclude that different wall boundary condition only contributes to a small change near the wall region. As we do not account for energy balance, and based on the recommendation of Andrews (2005), one chooses no slip boundary conditions for the solid phase.

The boundary condition for the inflow velocities at the bottom of the device is assumed to be uniform. The flux of the gas is determined by the superficial gas velocity reported by van den Moortel *et al.* (1998). The volume fraction of particle inflow is assumed to be 0.4, which is the value for the minimal fluidization conditions. The superficial velocity of the gas phase was 1 m/s for according to van den Moortel *et al.* (1998) data.

Simulations starts with the particles uniformly distributed in the fluidized bed and the velocities for both phases set to zero. The simulations were continued until about 15 seconds of real time. The statistical steady state was reached in

our simulations after about 2 seconds of real time, knowing that the characteristic time of the flow is 0.2 seconds and the relaxation time for the particle phase is 0.11 seconds, providing a Stokes number of 0.55 and a particle Reynolds number, Re_p~6.

For the gas phase the Kolmogorov length scale is h ~0.015 cm and the time scale is about of 0.002 seconds. Note that with this scales we do not resolve all the length scales for the gas flow. For the particle flow the grid size and time resolution is adequate to account for the presence of clusters and strands supported by the experimental results of Horio and Kuroki (1994).

5. NUMERICAL VERSUS EXPERIMENTAL RESULTS

Experimental results of van den Moortel *et al*. (1998) for the case of 1 m/s superficial gas velocity were used. We compare our averaged numerical results, 2s after start-up in the simulations. First we show the fine meso-scale structures, particle clusters and strands.

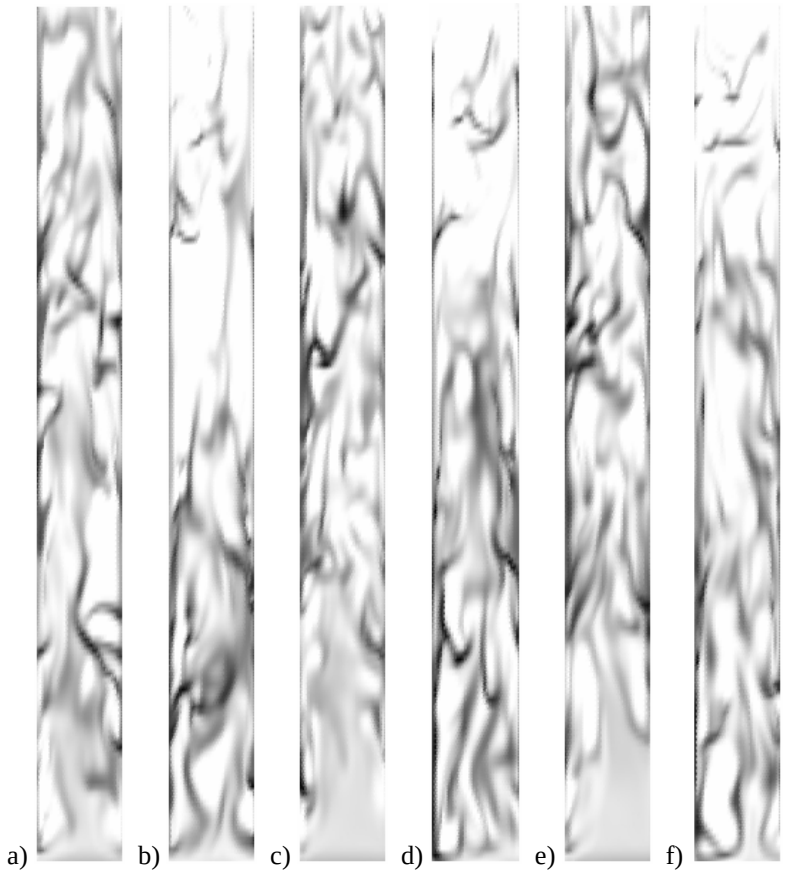

Figure 2. Particle volume fraction contours on a mid-plane (z=10 cm). Figures a), c) and e) denote Case 1, without sub-grid model, at 3.8, 4.0 and 4.2 seconds; Figures b), d) and f) denote Case 2, with sub-grid correction for both phases, at 3.8, 4.0 and 4.2 seconds. Gray scale represents particle agglomeration and white color represents gas phase.

Figure 2 shows simulations for two cases, Case 1, without using sub-grid model and Case 2 using sub-grid model for both phases. What we see in this figure is qualitatively similar to results obtained by Agrawal *el al*. (2001). The strands are thin and oriented in the axial direction and clusters are present near the wall. The bottom region of the bed is denser than the top region, characterizing a turbulent fluidized bed regime. We can see that strands do not stay only near the wall, appearing at the center of the bed, oriented some times in the lateral direction. Clusters and strands are continuously formed and destructed, giving rise to lateral fluctuations of the solid volume fraction. As the gas phase passes throughout the clusters it carries solid, forming new structures, but now more dilutes. Case 1 is denser near the bottom of the bed than Case 2, but for both cases the meso-scales are present and were adequately captured. For the Case 2 the structures appear thinner and the top of the bed is more dilute than Case 1.

As mentioned above, Agrawal *et al*. (2001) obtained computed meso-scale structures in their gas-solid flow simulations. There are, however, some key differences between their results and the one presented in this work. Agrawal *et al.* (2001) computed on a small two-dimensional 1cm x 4 cm periodic domain, which is much smaller than used in this work. While our smallest space increment was 0.625 cm, Agrawal *et al.* (2001) computed space increments

as fine as 0.016 cm. For larger mesh sizes, the numerical results significantly over-predict the particle mass flux, because the meso-scale structures are not resolved adequately by coarse grids, Geraldine *et al*. (2004). Inside a particle cluster the particle phase feels less drag since it falls in the "wake" generated by the leading part of the cluster. In the case of a coarse grid, this effect is not resolved, so particle drag is overestimated, Agrawal *et al.* (2001). This effect is more pronounced at dilute regions of the bed as we will see in our averaged results. However, the results presented in Fig 2, reveals qualitatively all meso-scale structures pointed out by Agrawal *et al.* (2001) and the characteristics of the turbulent fluidized bed regime are adequately represented.

The averaged results are calculated using Favre average of volume fraction and velocity of each phase, the same method used by van den Moortel *et al.* (1998) for their experiments, as follows

$$\overline{f_k} = \frac{\sum f_k \Delta t}{\sum \Delta t}, \tag{15}$$

$$\overline{u_{i,k}} = \frac{\sum f_k u_{i,k} \Delta t}{\sum f_k \Delta t}. \tag{16}$$

The subscript $i=g,p$ for the gas and the particle phase, respectively. Averaged velocity of each phase, defined above, is weighted by the volume fraction of the particle phase.

Figure 3 shows the averaged particle vertical velocity for Case 1 and 2. Calculated particle velocities agree with the trends of the experimental results overestimating the downward velocities near the wall, while in the center region (dilute) the agreement is good, Fig. 3 (a).

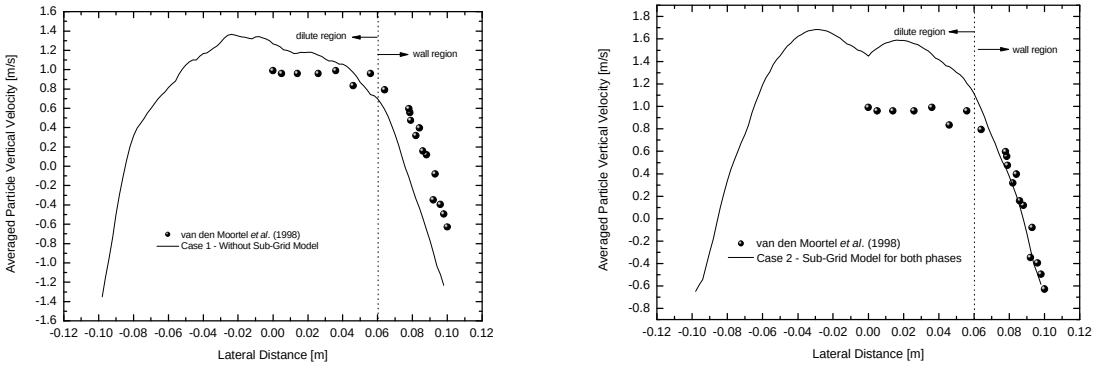

a) b)

Figure 3. a) Averaged particle vertical velocity profiles for Case 1 at z= 1m from the bottom of the bed; b) averaged particle vertical velocity profile for Case 2 at z= 1m form the bottom of the bed. Experimental results from van den Moortel *et al*. (1998).

When the results for Case 2 are compared with experiment, Fig. 3 (b), the particle velocities near the wall agree very well, however, at the dilute region the velocities are even more overestimated more than for Case 1. Comparing the results for Case 1 and 2 we see that the sub-grid model obtained a very good approximation at the dense region of the bed what does not occur when no sub-grid correction is applied.

These results show that the use of the sub-grid model can be appropriated according to the region of the flow. Near the wall we would use the sub-grid model, and at some distance from the dense region it could be used a modification of the present sub-grid model. We stress that we do not make any tests to modify the sub-grid constant (Eq. 6 and 8).

5.1 Power spectrum density

In this sub-section we show the power spectrum density (PSD) for the two cases studied. Figure 4 shows the total energy spectrum for Case 1, Fig. 4 (a), and the particle velocities fluctuation power spectrum density, Fig. 4 (b). As seen in Fig 4 (a), the total energy is greater at the central region than near wall, for the large length scale. The inertial zone begins around 0.4 Hertz for the center velocities and 0.2 Hertz for the wall. Similar frequency has been reported by Neri and Gidaspow (2000), using kinetic theory approach for particulate phase. This frequency represents the formation and destruction of cluster structures. These frequency oscillations of gas-solid flow could be used to know the minimum time required to conduct proper time averaging, which for our case is 5s. Note that we take averages over 13 s.

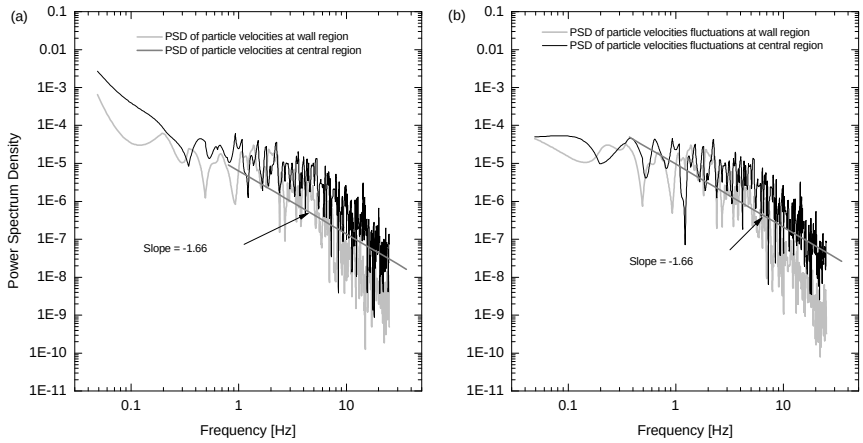

Figure 4. a) Power spectrum density of the simulated particle velocities for Case 1; b) Power spectrum density of the simulated particle velocities fluctuations for Case 1.

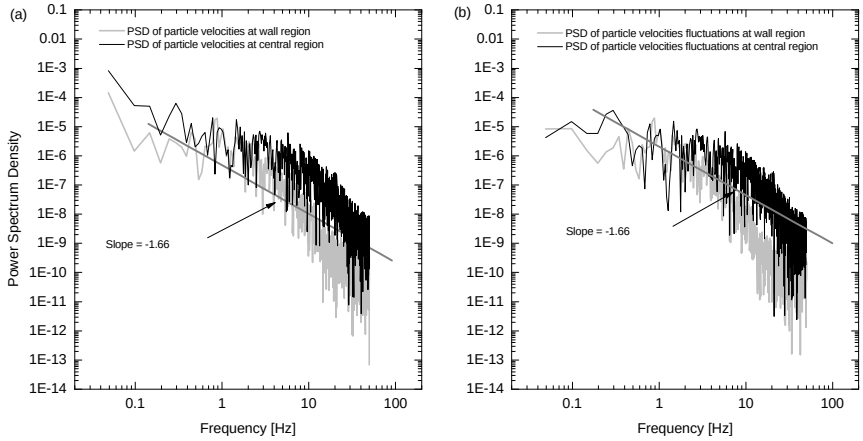

Figure 5. a) Power spectrum density of the simulated particle velocities for Case 2; b) Power spectrum density of the simulated particle velocities fluctuations for Case 2.

The power spectrum density for the fluctuation of the particles velocities for the central region, Fig. 4 (b), has more energy than for the wall region. The inertial region decay with -5/3 begins about 0.4 Hertz for the center and about 0.7 Hertz for the near wall region. The turbulent kinetic energy at central region is greater than wall region. From 10 Hertz the slope for the particle velocities PSDs at the wall is augmented significantly, indicating major dissipation at this region, where cluster are encountered with major frequency which contribute with the greater dissipation.

The Kolmogorov -5/3 law is obeyed in the inertial range, like the experimental results for gas-liquid-solid flow obtained by Cui and Fan (2004) with the same particle diameter used here and there obtained by Moran and Glicksman (2003) for the same particle diameter for gas-solid flow.

Figure 5 (a) shows the total spectrum of energy for the particle velocities at central and near wall regions for Case 2. The central region has more energy associated with large scale than wall region. Inertial sub-range begins about 0.45 Hertz for central region and 0.3 Hertz for wall with -5/3 decay. The power spectrum density of the velocities fluctuations, Fig 5 (b), has the same behavior as Case 1, Fig 4 (b). From 10 Hertz the dissipation of kinetic energy is major than Case 1 for near wall region. In both cases 1 and 2, at low frequencies, we see coherent structures represented by the great peaks. As the large scales structures are broken these peaks are smoothed to form the inertial region. The first peak appears about 0.3 Hertz representing the natural frequency of gas-solid flow in a fluidized bed.

The results presented in this section shows that the sub-grid model used was appropriate to represent the characteristics behaviors of gas-solid flow in a circulating fluidized bed, as mentioned above, especially near the wall region of the bed. The very good approximation of the averaged velocity to the experimental data near the wall for the

sub-grid model results, Case 2, shows the applicability of this methodology. The power spectrum density results are coherent with experimental data and the results obtained by kinetic theory.

6. CONCLUSIONS

Numerical simulations using the Two Fluid Model for multiphase flow were performed with the appropriate grid refinement to account meso-scale structures like clusters and strands. Comparisons were made with experimental results showing good agreement for certain regions of the flow using a sub-grid model. The outcome of the work suggests that Smagorinsky-like sub-grid model could be used in gas-solid flow with proper modifications for the dilute region of the circulating fluidized bed. Very good agreement for the near wall averaged particle velocities was found. The characteristic behavior of a turbulent fluidized bed was well represented with the bottom of the bed more dense than the top with clusters and strands presented in all locations of the bed. The results for the Case 1 showed that the bottom region of the bed was denser than for the Case 2.

Spectral profiles shows that the dissipation is greater near the wall and the decay of the power spectrum obey the Kolmogorov -5/3 law, indicating that the refinement in space and time was adequate. The natural frequency calculated by kinetic theory is captured.

Generally in gas-solid flows the particle viscosity is modeled as an empirically function of the particle volume fraction (e.g. Huilin *et al.* 2003). Results presented in Fig. 3 (a) for Case 1 (where the viscosity was maintained constant), suggest that this function is not needed for the fluidized bed studied here. For the Case 2 the viscosity was modeled with sub-grid corrections which are a function of the strain tensor. Results for Case 2, Figure 3 (b) shows a modified profile of the Favre averaged particle velocities in the central region when compared with the Favre averaged particle velocities for Case 1. Because the viscosities of Case 1 is constant and for Case 2 are not, we may conclude that the deviation of results for Case 2 is originated from this difference. As the stress for gas and solid phase, Eq. 5 and 7, are dependent on the volume fractions, we could conclude that the volume fraction already contribute to modify the stress and may not necessarily be included in the viscosity formulation.

It is important to mention that the averaged results for Case 1, Fig. 3 (a), suggests that a refinement of the grid will produce better results, dispensing the use of a sub-grid correction, but augmenting the computation cost.

7. ACKNOWLEDGEMENTS

The authors gratefully acknowledge the financial support for this work by the PRH09 - ANP/MCT (Agência Nacional de Petróleo, Gás e Biocombustíveis), through a scholarship for the first author.

8. REFERENCES

Andrews IV, A.T., Loeezos, P.N. and Sundaresan, S., 2005, “Coarse-grid Simulation of Gas-Particle Flows in Vertical Risers”, Ind. Eng. Chem. Res. Vol. 44, No. 16, pp. 6022-6037.

Agrawal K., Loezos, P.N, Syanmlal, M., Sundaresan, S., 2001, “The role of meso-scale structures in rapid gas-solid flows”, Journal of Fluid Mechanics, Vol. 445, pp. 151-185.

Anderson, J.D., 1995, “Computational Fluid Dynamics: The basics with applications. Mechanical Engineering Series. McGraw-Hill, New York.

Anderson, T.B, and Jackson, R., 1967, “A fluid mechanical description of fluidized beds. Ind. Engng. Chem. Fundam., Vol. 6, , No. 4, pp. 527-539.

Cui, Z. and Fan, L.S., 2004, “Turbulent energy distributions in bubbling gas-liquid and gas-liquid-solid flow systems”, Chemical Engineering Science, Vol. 59, pp. 1755-1766.

Gidaspow, D., 1994, “Multiphase Flow and Fluidization. Academic Press, San Diego, first edition.

Georg, I. C., 2005, “Modelagem e simulação numérica tridimensional transiente do escoamento gás-sólido em um reator de craqueamento catalítico em leito fluidizado”, PhD Dissertation, Departamento de Engenharia Mecanica da Universidade Federal de Santa Catarina.

Geraldine, J.H., Das, A. K., de Wilde, J., Marin, G.B., 2004, “Effect of Clustering on Gas-Solid Drag in Dilute Two-Phase Flow”, Ind. Eng. Chem. Res., Vol. 43, pp. 4635-4646.

Horio, M., Kuroki, H, 1994, “Three-Dimensional Flow Visualization of Dilutely Dispersed Solids in Bubbling and Circulating Fluidized Beds”, Chemical Engineering Science, Vol 49, pp. 2413-2421.

Huilin, L., Gidaspow, D., Bouillard, J., Wentie, L., 2003, “Hydrodynamic simulation of gas-solid flow in a riser using kinetic theory of granular flow”, Chemical Engineering Journal, Vol. 95, pp. 1-13.

Ishi, M., 1975, “Thermo-Fluid dynamic theory of Two-Phase Flow. Direction des etudes et Recherches d’Electricité de France. Paris, France.

Jackson, R., 1997, “Locally averaged equations of motion for mixture of identical spherical particles and a newtonian fluid”, Chem. Eng. Sci., Vol. 52, pp. 2457-2469.

Jackson, R., 2000, “The Dynamics of Fluidized Particles”, Cambridge University Press, Cambridge Monographs on Mechanics.

Moran, J.C. and Glicksman, L.R, 2003, “Mean and fluctuating gas phase velocities inside a circulating fluidized bed”, Chemical Engineering Science, Vol. 58, pp. 1867-1878.

Neri, A. Gidaspow, D., 2000, “Riser hydrodynamics: simulation using kinetic theory”, AIChe Journal, Vol. 46, pp. 52-67.

van den Moortel, T. Azario, E., Santini, R., Tadrist, L., 1998, “Experimental analysis of the gas-particle flow in a circulating fluidized bed using a phase Doppler particle analyzer”, Chemical Engineering Science, Vol. 53, , No. 10, pp. 1883-1899.

van Wachem, B., 2000, “Derivation, Implementation, and Validation fo Computer Simulation Models for Gas-Solid Fluidized Beds”, PhD Dissertation, Delft University of Technology.

Zhang, D.Z., van der Heyden, W.B., 2001, “High-resolution three-dimensional numerical simulation of a circulating fluidized bed”, Powder Technology, Vol. 116, pp. 133-141.

9. RESPONSIBILITY NOTICE

The author(s) is (are) the only responsible for the printed material included in this paper.